Hamburger Beiträge
zur Angewandten Mathematik

Image Reconstruction from Scattered Radon Data by Weighted Positive Definite Kernel Functions

S. De Marchi, A. Iske, G. Santin

Nr. 2017- 02
January 2017

Image Reconstruction from Scattered Radon Data by Weighted Positive Definite Kernel Functions

S. De Marchi · A. Iske · G. Santin

January 25, 2017

Abstract We propose a novel kernel-based method for image reconstruction from scattered Radon data. To this end, we employ generalized Hermite-Birkhoff interpolation by positive definite kernel functions. For radial kernels, however, a straightforward application of the generalized Hermite-Birkhoff interpolation method fails to work, as we prove in this paper. To obtain a well-posed reconstruction scheme for scattered Radon data, we introduce a new class of *weighted* positive definite kernels, which are symmetric but not radially symmetric. By our construction, the resulting weighted kernels are combinations of radial positive definite kernels and positive weight functions. This yields very flexible image reconstruction methods, which work for arbitrary distributions of Radon lines. We develop suitable representations for the weighted basis functions and the symmetric positive definite kernel matrices that are resulting from the proposed reconstruction scheme. For the relevant special case, where Gaussian radial kernels are combined with Gaussian weights, explicit formulae for the weighted Gaussian basis functions and the kernel matrices are given. Supporting numerical examples are finally presented.

Keywords Image reconstruction · kernel-based approximation · generalized Hermite-Birkhoff interpolation · Radon transform · positive definite kernels

Stefano De Marchi
Department of Mathematics, University of Padua, Italy
E-mail: demarchi@math.unipd.it

Armin Iske
Department of Mathematics, University of Hamburg, Germany
E-mail: iske@math.uni-hamburg.de

Gabriele Santin
Institute of Applied Analysis and Numerical Simulation, University of Stuttgart, Germany
E-mail: gabriele.santin@mathematik.uni-stuttgart.de

1 Introduction

Computed Axial Tomography (CAT or CT) is a powerful technique to generate images from measurements of X-ray scans. One X-ray scan typically consists of several million of data samples, each of which corresponds to an X-ray beam passing through the computational domain, travelling from an emitter to a detector. The sensors of the operational CT scanner (positioned at the emitter and at the detector) then measures, for each X-ray beam, the loss of energy, resulting from the X-ray beam passing through the medium. The loss of energy reflects the ability of the medium to absorb energy, and so it depends on its specific structure and material properties. The amount of absorption can be described as a function of the computational domain Ω, termed *attenuation coefficient function*, $f : \Omega \to [0, \infty)$.

But medical imaging is only one relevant application for CT, where the primary goal is to reconstruct the unknown attenuation coefficient function f from given X-ray scans in order to generate clinically useful medical images. Other relevant applications are e.g. non-destructive evaluations of materials. In either case, robust numerical algorithms are required to reconstruct characteristic features of images at sufficiently high accuracy, on the one hand, and at sufficiently small computational costs, on the other hand. For details concerning the acquisition of X-ray scans, their underlying mathematical models, and standard computational methods for medical image reconstruction, we refer to the textbook [5] of Feeman.

To briefly describe the mathematical problem of medical image reconstruction from X-ray scans, we first regard the *Radon transform* $\mathcal{R}f$ of f, given by

$$\mathcal{R}f(t,\theta) = \int_{\mathbb{R}} f(t\cos\theta - s\sin\theta, t\sin\theta + s\cos\theta)\,\mathrm{d}s \tag{1}$$

for $(t,\theta) \in \mathbb{R} \times [0,\pi)$, where we assume $f : \Omega \to \mathbb{R}$ to be a bivariate function on a compact domain $\Omega \subset \mathbb{R}^2$, or, we assume that f is compactly supported on $\mathbb{R}^2$, where we extend f to $\mathbb{R}^2$ by letting $f \equiv 0$ outside Ω. In our numerical experiments, we assume a square image domain $\Omega = [-1,1]^2$, but this restriction is rather immaterial for our following discussion. We merely assume $f \in \mathrm{L}^1(\mathbb{R}^2)$, so that for any pair of $t \in \mathbb{R}$ and $\theta \in [0,\pi)$ the Radon integral in (1) is well-defined.

We remark that the Radon transform $\mathcal{R}f(t,\theta)$ gives, for any fixed pair $(t,\theta) \in \mathbb{R} \times [0,\pi)$, a line integral for f over a specific straight line $\ell \equiv \ell_{t,\theta}$. In order to see this, let $\ell_{t,\theta} \subset \mathbb{R}^2$ denote the unique straight line, which is perpendicular to the unit vector $\mathbf{n}_\theta = (\cos\theta, \sin\theta)$ and which passes through the point $p = (t\cos\theta, t\sin\theta) = t\mathbf{n}_\theta$. In this case, the line $\ell_{t,\theta}$ can be parameterized as

$$(x_1(s), x_2(s)) = (t\cos\theta - s\sin\theta, t\sin\theta + s\cos\theta) \qquad \text{for } s \in \mathbb{R}. \tag{2}$$

By this specific choice for a parameterization of $\ell_{t,\theta}$ in (2), we see that

$$\mathcal{R}f(t,\theta) = \int_{\ell_{t,\theta}} f(\mathbf{x})\,\mathrm{d}\mathbf{x} \qquad \text{for } (t,\theta) \in \mathbb{R} \times [0,\pi),$$

where we let $\mathbf{x} = (x_1, x_2)$, and so the line integral of f over $\ell_{t,\theta}$ coincides with the Radon transform (1) of f at (t, θ).

On the other hand, any straight line ℓ in the plane can be described by a unique pair (t, θ) of a radial parameter $t \in \mathbb{R}$ and an angular parameter $\theta \in [0, \pi)$ satisfying $\ell \equiv \ell_{t,\theta}$. In this way, the Radon transform $\mathcal{R}f$ of f can be viewed as a transformation, which maps any bivariate function $f \in \mathrm{L}^1(\mathbb{R}^2)$ (in Cartesian coordinates) onto a bivariate function $\mathcal{R}f$ (in polar coordinates), where the image $\mathcal{R}f$ contains all line integrals of f over the set of straight lines in the plane.

Due the seminal work [12] of Johann Radon, any $f \in \mathrm{L}^1(\mathbb{R}^2) \cap \mathscr{C}(\mathbb{R}^2)$ can be reconstructed from its Radon transform $\mathcal{R}f$. The inversion of the Radon transform is given by the *filtered back projection* (FBP) formula (see [5, Chapter 6]),

$$f(\mathbf{x}) = \frac{1}{2}\mathcal{B}\left\{\mathcal{F}^{-1}\left[|S|\mathcal{F}(\mathcal{R}f)(S,\theta)\right]\right\}(\mathbf{x}), \tag{3}$$

where $\mathcal{F}$ is, for any fixed angle θ, the *univariate* Fourier transform w.r.t. the radial variable t, and so is $\mathcal{F}^{-1}$ the univariate inverse Fourier transform w.r.t. the frequency variable S. Moreover, the *back projection* $\mathcal{B}$ is, for any function $h \equiv h(t, \theta)$ (in polar coordinates), given by the average

$$\mathcal{B}h(\mathbf{x}) = \frac{1}{\pi}\int_0^\pi h(x_1\cos\theta + x_2\sin\theta, \theta)\,\mathrm{d}\theta$$

of $h(t, \theta)$ over the angular variable θ, where we let

$$t = x_1\cos\theta + x_2\sin\theta = \mathbf{x}\cdot\mathbf{n}_\theta$$

according to the one-to-one relation between the polar coordinates (t, θ) and the Cartesian coordinates $\mathbf{x} = (x_1, x_2)$, as described above along with the parameterization of the lines $\ell_{t,\theta}$ in (2). For basic details concerning the derivation of the filtered back projection formula, we refer to [5], and for a more comprehensive mathematical treatment of the Radon transform and its inversion, we refer to the textbooks [7, 11].

In practical application scenarios, however, only a *finite* set of Radon data,

$$\mathcal{R}_\mathcal{L}(f) = \{\mathcal{R}f(t_k, \theta_k)\}_{k=1}^m, \tag{4}$$

given as integrals of f over a finite set of m pairwise distinct lines,

$$\mathcal{L} = \{\ell_{t_k,\theta_k} : (t_k, \theta_k) \in \mathbb{R}\times[0,\infty) \text{ for } k = 1, \ldots, m\},$$

is available. In this case, an approximate reconstruction of f from Radon data $\mathcal{R}_\mathcal{L}f$ is sought. In standard techniques of medical imaging, the reconstruction of f is accomplished by using a suitable discretization of the FBP in (3). For this class of Fourier-based reconstruction methods, the discrete lines in $\mathcal{L}$, over which the line integrals of f are known, are usually required to be regularly spaced in the plane, e.g. by assuming *parallel beam geometry* or *fan beam geometry* (see [5] for particular assumptions on the geometry of $\mathcal{L}$).

In many realistic scenarios of data acquisition, however, we may face a limited range of angles (e.g. in mammography), or a limited dosage of X-ray expositions, so that the Radon data are partly corrupt or incomplete. In such relevant cases, the Radon data in (4) are *scattered*, i.e., the distribution of lines in $\mathcal{L}$ is essentially *not* regular but scattered, in which case standard Fourier methods, such as the Fourier-based FBP discretization in (3), do no longer apply. This requires more flexible approximation methods which work for arbitrary geometries of (scattered) Radon lines $\mathcal{L}$.

To approximate f from *scattered* Radon data $\mathcal{R}_{\mathcal{L}} f$, *algebraic reconstruction techniques* (ART) [6] can be applied. The concept of ART is essentially different from that of Fourier-based reconstructions: in the setting of ART one fixes a set $\mathcal{G} = \{g_j\}_{j=1}^n$ of basis functions beforehand to solve the reconstruction problem

$$\mathcal{R}_{\mathcal{L}}(g) = \mathcal{R}_{\mathcal{L}}(f) \tag{5}$$

by using a linear combination

$$g = \sum_{j=1}^{n} c_j g_j$$

of the basis functions. This assumption amounts to solving the linear system

$$Ac = b \tag{6}$$

for the unknown coefficients $c = (c_1, \ldots, c_n)^T \in \mathbb{R}^n$ of g, where the $m \times n$ matrix A has the form

$$A = \left(\mathcal{R} g_j(t_k, \theta_k)\right)_{k=1,\ldots,m; j=1,\ldots,n} \in \mathbb{R}^{m \times n} \tag{7}$$

and where $b = (b_1, \ldots, b_m)^T \in \mathbb{R}^m$ is given by the m Radon observations $b_k = \mathcal{R} f(t_k, \theta_k)$, for $k = 1, \ldots, m$.

Unless the number m of Radon samples coincides with the number n of coefficients, the linear system in (6) is either overdetermined, for $m > n$, or underdetermined, for $n > m$. In case of an overdetermined system, the classical method of *linear least squares approximation* [2] is applied to minimize the residual (Euclidean) norm $\|Ac - b\|$, whereas for an underdetermined system the iterative method of Kaczmarz [5, Section 9.3] is a standard tool to compute an approximate solution c satisfying $Ac \approx b$. We remark that in either case the linear system in (6) is not guaranteed to have a unique solution, not even when $m = n$. In fact, the latter is due to the *Mairhuber-Curtis theorem* [15, Section 2.1] from multivariate approximation theory.

A first kernel-based approach for scattered data interpolation from Radon data was developed in [1]. The resulting kernel method in [1] transfers the reconstruction problem (5) into one for suitable projective spaces, on which positive definite zonal functions are utilized to accomplish the recovery step. We remark that the straightforward approach taken in this paper is essentially different from that in [1], although [1] relies on positive definite kernels, too.

In previous work [4], we considered using radially symmetric kernels in combination with regularizations of the Radon transform. The approach taken in [4], however, leads to linear systems (6) with unsymmetric matrices A. In this paper, we propose a well-posed kernel-based reconstruction method, whose resulting kernel matrices $A \in \mathbb{R}^{n\times n}$ are symmetric and positive definite. Our proposed reconstruction scheme relies on the theory of kernel-based multivariate interpolation from generalized Hermite-Birkhoff data [9]. We adapt this particular interpolation scheme to the special case of image reconstruction from scattered Radon data. In this case, the basis functions in $\mathcal{G} = \{g_j\}_{j=1}^n$ must essentially depend on the given Radon functionals $\mathcal{R}_\mathcal{L}$. We show that an uncustomized application of generalized Hermite-Birkhoff reconstruction fails to work for radially symmetric kernels. To guarantee the well-posedness of the reconstruction scheme, particularly to obtain well-defined entries in A, we develop a general concept for the construction of *weighted* positive definite kernels. The resulting kernels are symmetric but not radially symmetric. We give examples for suitable pairs of radial weights and radial positive definite functions. This yields a new class of flexible reconstruction schemes, which work for arbitrary distributions of scattered Radon lines.

The outline of this paper is as follows. In Section 2, we briefly review generalized Hermite-Birkhoff interpolation, where we show how to adapt this particular reconstruction method to scattered Radon data. In Section 3, we introduce weighted radial kernels, where we explain how they are used to obtain a well-posed reconstruction method. Moreover, we develop suitable representations for the resulting basis functions g_j and the matrix entries for A in (7). This is followed by a discussion concerning one special case, where standard Gaussian kernels are combined with Gaussian weights. For this prototypical case, covered in Section 4, we give explicit formulae for the resulting Gaussian basis functions g_j and the Gaussian matrix entries a_{kj}. For the purpose of illustration, numerical results are finally provided in Section 5.

2 Generalized Hermite-Birkhoff Interpolation

To solve the reconstruction problem (5), we consider applying Hermite-Birkhoff interpolation [9]. To explain the general framework of this particular interpolation method, let $\Lambda = \{\lambda_1, \ldots, \lambda_n\}$ denote a set of linearly independent linear functionals. Moreover, suppose we are given a vector

$$f_\Lambda = (\lambda_1(f), \ldots, \lambda_n(f))^T \in \mathbb{R}^n$$

of samples taken from an unknown function f. Now the solution of the general Hermite-Birkhoff reconstruction problem requires finding a function g satisfying the interpolation conditions $g_\Lambda = f_\Lambda$, i.e.,

$$\lambda_k(g) = \lambda_k(f) \qquad \text{for all } k = 1, \ldots, n. \tag{8}$$

This general framework covers our reconstruction problem (5), when the linear functionals λ_k are defined as

$$\lambda_k(f) := \mathcal{R}_k f \equiv \mathcal{R} f(t_k, \theta_k) \qquad \text{for } k = 1, \ldots, n.$$

By the interpolation conditions in (8), we obtain n linear equations,

$$\sum_{j=1}^{n} c_j \lambda_k(g_j) = \lambda_k(f) \qquad \text{for } k = 1, \ldots, n,$$

corresponding to the linear system in (6), where the number of equations matches the number of basis functions, i.e., $n = m$.

Following along the lines of the Hermite-Birkhoff interpolation scheme, the basis functions g_j are assumed to have the form

$$g_j(\mathbf{x}) = \lambda_j^{\mathbf{y}} K(\mathbf{x}, \mathbf{y}) \qquad \text{for } j = 1, \ldots, n, \tag{9}$$

where $\lambda_j^{\mathbf{y}} K(\mathbf{x}, \mathbf{y})$ denotes the action of the functional λ_j to K w.r.t. variable $\mathbf{y} \in \mathbb{R}^2$. Moreover, the kernel function $K \equiv K(\mathbf{x}, \mathbf{y})$ is required to be *symmetric*, i.e.,

$$K(\mathbf{x}, \mathbf{y}) = K(\mathbf{y}, \mathbf{x}) \quad \text{for all } \mathbf{x}, \mathbf{y} \in \mathbb{R}^2,$$

and *positive definite*.

Rather than dwelling much on explaining positive definite functions, we remark that for the purposes of this paper it is sufficient to say that a symmetric function $K \equiv K(\mathbf{x}, \mathbf{y})$ is *positive definite*, iff the matrix

$$A_{K,\Lambda} = \left(\lambda_j^{\mathbf{x}} \lambda_k^{\mathbf{y}} K(\mathbf{x}, \mathbf{y})\right)_{1 \le j,k \le n} \in \mathbb{R}^{n \times n} \tag{10}$$

is symmetric positive definite for any set $\Lambda = \{\lambda_j\}_{j=1}^n$ of linearly independent functionals λ_j. For a comprehensive account to the construction and characterization of positive definite kernels, we refer the reader to [10, 13].

Before we make concrete examples for suitable (symmetric and positive definite) kernels K, the following remarks are in order.

Remark 1 For the special case of plain Lagrange interpolation, i.e., interpolation from point values, commonly used kernels K are *radially symmetric*,

$$K_\phi(\mathbf{x}, \mathbf{y}) = \phi(\|\mathbf{x} - \mathbf{y}\|^2) \qquad \text{for } \mathbf{x}, \mathbf{y} \in \mathbb{R}^2,$$

where ϕ is continuous and radial w.r.t. the Euclidean norm $\|\cdot\|$. □

Among the most prominent examples for radially symmetric kernels are the *Gaussians*

$$\phi_\alpha(\|\mathbf{x}\|^2) = \mathrm{e}^{-\alpha\|\mathbf{x}\|^2} \quad \text{for } \mathbf{x} \in \mathbb{R}^2$$

that are for any $\alpha > 0$ positive definite, i.e.,

$$K(\mathbf{x}, \mathbf{y}) = \exp(-\alpha\|\mathbf{x} - \mathbf{y}\|^2)$$

is positive definite. Other popular examples are the *inverse multiquadrics*,

$$\phi_\alpha(\|\mathbf{x}\|^2) = \big(1+\alpha\|\mathbf{x}\|^2\big)^\beta \qquad \text{for } \mathbf{x}\in\mathbb{R}^2 \text{ and } \alpha>0,$$

which are positive definite for any $\beta \in (-1,0)$.

Remark 2 For the special case of Radon data, however, the selection of a suitable kernel requires particular care. To further explain this, note that the reconstruction method can only work, if the basis functions g_j in (9) are well-defined, and, moreover, all entries in matrix A in (10) are well-defined. To guarantee well-defined basis functions g_j, we merely require

$$\phi(\|\mathbf{x}-\cdot\|^2) \in \mathrm{L}^1(\mathbb{R}^2) \qquad \text{for all } \mathbf{x}\in\mathbb{R}^2.$$

Note that this property is satisfied by the Gaussians, but not by the inverse multiquadrics, and so one could argue this is only a minor problem. The other point concerning well-defined entries in A is, indeed, more severe. □

To further explain this problem, let us provide the following negative result.

Proposition 1 *Let $\phi(\|\cdot\|^2):\mathbb{R}^2\to[0,\infty)$ be continuous and positive definite on $\mathbb{R}^2$, and let $\ell\subset\mathbb{R}^2$ be a straight line in the plane. Then the integral*

$$\int_\ell\int_\ell \phi(\|\mathbf{x}-\mathbf{y}\|^2)\,\mathrm{d}\mathbf{x}\,\mathrm{d}\mathbf{y}$$

is divergent.

Proof Without loss of generality, let $\ell=\{(x,0):x\in\mathbb{R}\}$ be aligned with the x-axis. We can assume this because $\phi(\|\mathbf{x}-\mathbf{y}\|^2)$ is invariant under rotations and translations. In this case,

$$I := \int_\ell\int_\ell \phi(\|\mathbf{x}-\mathbf{y}\|^2)\,\mathrm{d}\mathbf{x}\,\mathrm{d}\mathbf{y} = \int_{\mathbb{R}}\int_{\mathbb{R}} \phi(|x-y|^2)\,\mathrm{d}x\,\mathrm{d}y.$$

Now assume that the integral I is finite. Then, we have

$$\int_{\mathbb{R}}\int_{\mathbb{R}} \phi(|x-y|^2)\,\mathrm{d}x\,\mathrm{d}y > \int_{D_\varepsilon^L} \phi(|x-y|^2)\,\mathrm{d}x\,\mathrm{d}y > \phi(\varepsilon^2)\mathrm{vol}_2(D_\varepsilon^L), \qquad (11)$$

where D_ε^L denotes, for any $L>0$ and $\varepsilon>0$, the diagonal strip

$$D_\varepsilon^L := \{(x,y)\in[-L,L]^2 : |x-y|\le\varepsilon\}\subset\mathbb{R}^2,$$

and where $\varepsilon>0$ is chosen small enough to guarantee $\phi(\varepsilon)>0$. In the above inequality (11), we use that the (non-negative) positive definite ϕ attains its unique maximum at the origin.

Now since, for fixed $\varepsilon>0$, the area $\mathrm{vol}_2(D_\varepsilon^L)$ may be arbitrarily large, i.e., $\mathrm{vol}_2(D_\varepsilon^L)\to\infty$, for $L\to\infty$, this is in contradiction to our assumption, and so the integral on the left hand side in (11) cannot be finite. □

In conclusion, the above proposition states that for any radially symmetric kernel $K_\phi(\mathbf{x},\mathbf{y}) = \phi(\|\mathbf{x}-\mathbf{y}\|^2)$, the diagonal entries of the matrix $A_{K,\Lambda}$ in (10) are (for the case of Radon functionals) *singular*, as they are given by

$$\mathcal{R}_k^{\mathbf{x}}\mathcal{R}_k^{\mathbf{y}}\phi(\|\mathbf{x}-\mathbf{y}\|^2) = \int_{\ell_k}\int_{\ell_k} \phi(\|\mathbf{x}-\mathbf{y}\|^2)\,\mathrm{d}\mathbf{x}\,\mathrm{d}\mathbf{y}$$

for straight lines $\ell_k \subset \mathbb{R}^2$, $1 \le k \le n$. In this case, an uncustomized application of generalized Hermite-Birkhoff interpolation is therefore doomed to fail.

3 Weighted Positive Definite Kernels

Unlike in standard applications of kernel-based approximation, where the utilized kernel $K_\phi(\mathbf{x},\mathbf{y}) = \phi(\|\mathbf{x}-\mathbf{y}\|^2)$ is radially symmetric, we prefer to work with *weighted* kernels of the form

$$K_{\phi,w}(\mathbf{x},\mathbf{y}) = \phi(\|\mathbf{x}-\mathbf{y}\|^2)w(\|\mathbf{x}\|^2)w(\|\mathbf{y}\|^2) \qquad \text{for } \mathbf{x},\mathbf{y}\in\mathbb{R}^2, \tag{12}$$

where $w : [0,\infty) \to (0,\infty)$ is a *weight function*. Note that $K_{\phi,w}$ in (12) is symmetric, but not radially symmetric.

The choice of $K_{\phi,w}$ in (12) will, for suitably chosen weights w, guarantee both well-defined basis functions g_j in (9) and well-defined matrix entries in (10). To this end, we show that $K_{\phi,w}$ in (12) is positive definite w.r.t. the *Schwartz space*

$$\mathcal{S} := \left\{\gamma \in \mathscr{C}^\infty(\mathbb{R}^d;\mathbb{R}) : D^p\gamma(\mathbf{x})\mathbf{x}^q \to 0 \text{ for all } p,q\in\mathbb{N}_0^d\right\}$$

of all rapidly decaying $\mathscr{C}^\infty$ functions [8,9].

Definition 1 A continuous and symmetric function $K : \mathbb{R}^d\times\mathbb{R}^d \to \mathbb{R}$ is said to be `positive definite` on $\mathcal{S}$, $K \in \mathbf{PD}(\mathcal{S})$, iff the double integral

$$\int_{\mathbb{R}^d}\int_{\mathbb{R}^d} K(\mathbf{x},\mathbf{y})\gamma(\mathbf{x})\gamma(\mathbf{y})\,\mathrm{d}\mathbf{x}\,\mathrm{d}\mathbf{y} \tag{13}$$

is positive for all $\gamma \in \mathcal{S}\setminus\{0\}$. □

The following observation will be important for our subsequent analysis.

Proposition 2 *Let $K \equiv K_\Phi : \mathbb{R}^d\times\mathbb{R}^d \to \mathbb{R}$ be of the form*

$$K_\Phi(\mathbf{x},\mathbf{y}) = \Phi(\mathbf{x}-\mathbf{y}) \qquad \textit{for } \mathbf{x},\mathbf{y}\in\mathbb{R}^d, \tag{14}$$

for an even function $\Phi \in \mathrm{L}^1(\mathbb{R}^d,\mathbb{R})\cap\mathscr{C}(\mathbb{R}^d,\mathbb{R})$. If K_Φ is positive definite on $\mathcal{S}$, $K_\Phi \in \mathbf{PD}(\mathcal{S})$, then the Fourier transform

$$\hat{\Phi}(\mathbf{z}) = \int_{\mathbb{R}^d} \Phi(\mathbf{x})\,\mathrm{e}^{-\mathrm{i}\mathbf{x}^T\mathbf{z}}\,\mathrm{d}\mathbf{x} \qquad \textit{for } \mathbf{z}\in\mathbb{R}^d$$

is positive on $\mathbb{R}^d$, i.e., $\hat{\Phi}(\mathbf{z}) > 0$ for all $\mathbf{z}\in\mathbb{R}^d$.

Proof By our assumptions on Φ, we can rely on the *Fourier inversion theorem*,

$$\Phi(\mathbf{x}-\mathbf{y}) = (2\pi)^{-d} \int_{\mathbb{R}^d} \hat{\Phi}(\mathbf{z}) \mathrm{e}^{\mathrm{i}(\mathbf{x}-\mathbf{y})^T\mathbf{z}} \,\mathrm{d}\mathbf{z}\,,$$

so that, for any $\gamma \in \mathcal{S}$, we find the representation

$$\begin{aligned}\int_{\mathbb{R}^d}\int_{\mathbb{R}^d} K_\Phi(\mathbf{x},\mathbf{y})\gamma(\mathbf{x})\gamma(\mathbf{y})\,\mathrm{d}\mathbf{x}\,\mathrm{d}\mathbf{y} &= \int_{\mathbb{R}^d}\int_{\mathbb{R}^d} \Phi(\mathbf{x}-\mathbf{y})\gamma(\mathbf{x})\gamma(\mathbf{y})\,\mathrm{d}\mathbf{x}\,\mathrm{d}\mathbf{y} \\ &= (2\pi)^{-d} \int_{\mathbb{R}^d} \hat{\Phi}(\mathbf{z}) \left(\int_{\mathbb{R}^d} \gamma(\mathbf{x}) \mathrm{e}^{-\mathrm{i}\mathbf{x}^T\mathbf{z}} \,\mathrm{d}\mathbf{x} \right)^2 \mathrm{d}\mathbf{z} \\ &= (2\pi)^{-d} \int_{\mathbb{R}^d} \hat{\Phi}(\mathbf{z}) \left|\hat{\gamma}(\mathbf{z})\right|^2 \,\mathrm{d}\mathbf{z}.\end{aligned}$$

From this we see that $\hat{\Phi}$ is positive on $\mathbb{R}^d$, since the double integral in (13) is assumed to be positive for all $\gamma \in \mathcal{S} \setminus \{0\}$. □

From now we will say that Φ in (14) is *positive definite* on $\mathcal{S}$, $\Phi \in \mathbf{PD}(\mathcal{S})$, iff $K_\Phi \in \mathbf{PD}(\mathcal{S})$. We can draw the following conclusion from Proposition 2.

Corollary 1 *Let $\Phi \in \mathrm{L}^1(\mathbb{R}^d,\mathbb{R}) \cap \mathscr{C}(\mathbb{R}^d,\mathbb{R})$ be even and positive definite on $\mathcal{S}$. Moreover, let $w : \mathbb{R}^d \to (0,\infty)$ be a continuous function of at most polynomial growth around infinity. Then, the function*

$$K_{\Phi,w}(\mathbf{x},\mathbf{y}) = \Phi(\mathbf{x}-\mathbf{y})w(\mathbf{x})w(\mathbf{y}) \qquad \textit{for } \mathbf{x},\mathbf{y} \in \mathbb{R}^d$$

is symmetric and positive definite on $\mathcal{S}$.

Proof Like in the proof of Proposition 2, we can establish the representation

$$\begin{aligned}\int_{\mathbb{R}^d}\int_{\mathbb{R}^d} K_{\Phi,w}(\mathbf{x},\mathbf{y})\gamma(\mathbf{x})\gamma(\mathbf{y})\,\mathrm{d}\mathbf{x}\,\mathrm{d}\mathbf{y} &= \int_{\mathbb{R}^d}\int_{\mathbb{R}^d} \Phi(\mathbf{x}-\mathbf{y})w(\mathbf{x})\gamma(\mathbf{x})w(\mathbf{y})\gamma(\mathbf{y})\,\mathrm{d}\mathbf{x}\,\mathrm{d}\mathbf{y} \\ &= (2\pi)^{-d} \int_{\mathbb{R}^d} \hat{\Phi}(\mathbf{z}) \left|\widehat{w\gamma}(\mathbf{z})\right|^2 \,\mathrm{d}\mathbf{z}. \qquad (15)\end{aligned}$$

Recall $\hat{\Phi} > 0$ from Proposition 2. Moreover, since w is positive on $\mathbb{R}^d$, the integral in (15) is positive for all $\gamma \in \mathcal{S} \setminus \{0\}$, and so $K_{\Phi,w} \in \mathbf{PD}(\mathcal{S})$. □

We remark that any positive definite function K on $\mathcal{S}$, $K \in \mathbf{PD}(\mathcal{S})$, is also positive definite on $\mathbb{R}^d$, $K \in \mathbf{PD}(\mathbb{R}^d)$. In other words, $K \in \mathbf{PD}(\mathcal{S})$ generates, for any set $\mathbf{X} = \{\mathbf{x}_1,\ldots,\mathbf{x}_n\} \subset \mathbb{R}^d$ of pairwise distinct points, a symmetric positive definite *kernel matrix*

$$A_{K,\mathbf{X}} = (K(\mathbf{x}_j,\mathbf{x}_k))_{1\le j,k\le n} \in \mathbb{R}^{n\times n},$$

by point evaluations of $K(\mathbf{x},\mathbf{y})$ at $\mathbf{X}\times\mathbf{X}$, and so we have

$$\mathbf{PD}(\mathcal{S}) \subset \mathbf{PD}(\mathbb{R}^d).$$

As shown in [8,9], the above inclusion is a rather straightforward consequence from the celebrated Bochner theorem [3], several of whose variants were used

to construct positive definite radial kernels — "radial basis functions" — for the purpose of multivariate approximation from Lagrange data [13].

In the situation of this paper, we wish to work with positive definite kernels $K \in \mathbf{PD}(\mathcal{S})$, all of whose kernel matrices

$$A_{K,\mathcal{L}} = \left(\mathcal{R}^{\mathbf{x}}_{\ell_j}\mathcal{R}^{\mathbf{y}}_{\ell_k}K(\mathbf{x},\mathbf{y})\right) \in \mathbb{R}^{n\times n}, \tag{16}$$

generated by integrals along a set of pairwise distinct Radon lines,

$$\mathcal{L} = \{\ell_1,\ldots,\ell_n\} \subset \mathbb{R}^2\,,$$

are symmetric positive definite. We call such kernels K positive definite with respect to the Radon transform $\mathcal{R}$, or, in short, $K \in \mathbf{PD}(\mathcal{R})$. As shown in Proposition 1, the class $\mathbf{PD}(\mathcal{R})$ contains no radially symmetric function K.

Therefore, we use weighted positive definite kernels $K_{\phi,w}$ of the form (12). Now the well-posedness of the resulting reconstruction scheme follows from [9]. For the reader's convenience, we summarize our discussion as follows.

Theorem 1 *Let $K_\phi(\mathbf{x},\mathbf{y}) = \phi(\|\mathbf{x}-\mathbf{y}\|^2)$ be a positive definite function on $\mathcal{S}$, $K_\phi \in \mathbf{PD}(\mathcal{S})$, and let $w : [0,\infty) \to (0,\infty)$ be continuous and positive. Moreover, suppose*

$$(\phi w)(|\cdot|^2) \in \mathrm{L}^1([0,\infty),\mathbb{R}).$$

Then, $K_{\phi,w}$ in (12) is positive definite w.r.t. $\mathcal{R}$, i.e., $K_{\phi,w} \in \mathbf{PD}(\mathcal{R})$. □

In the remainder of this section, we develop for weighted kernels $K_{\phi,w}$ of the form (12) suitable representations for their associated basis functions

$$g_{t,\theta}(\mathbf{x}) = \mathcal{R}^{\mathbf{y}}_{\ell_{t,\theta}}K_{\phi,w}(\mathbf{x},\mathbf{y}) \qquad \text{for } \ell_{t,\theta} \in \mathcal{L} \tag{17}$$

and for their matrix entries

$$a_{kj} = \mathcal{R}^{\mathbf{x}}_{\ell_j}\mathcal{R}^{\mathbf{y}}_{\ell_k}K_{\phi,w}(\mathbf{x},\mathbf{y}) \qquad \text{for } \ell_j,\ell_k \in \mathcal{L}. \tag{18}$$

3.1 Representation of the Weighted Basis Functions

For $K_{\phi,w}$ in (12), the weighted basis functions in (17) have the form

$$g_{t,\theta}(\mathbf{x}) = \mathcal{R}^{\mathbf{y}}_{t,\theta}\left[\phi(\|\mathbf{x}-\mathbf{y}\|^2)w(\|\mathbf{y}\|^2)\right]\cdot w(\|\mathbf{x}\|^2)\,, \tag{19}$$

where $\mathcal{R}_{t,\theta}$ is the Radon transform on line $\ell \equiv \ell_{t,\theta}$ for $(t,\theta) \in \mathbb{R}\times[0,\pi)$.

To compute $g_{t,\theta}(\mathbf{x}) = h_{t,\theta}(\mathbf{x})\cdot w(\|\mathbf{x}\|^2)$, we represent its major part as

$$\begin{aligned}
h_{t,\theta}(\mathbf{x}) &= \mathcal{R}^{\mathbf{y}}_{t,\theta}\left[\phi(\|\mathbf{x}-\mathbf{y}\|^2)w(\|\mathbf{y}\|^2)\right]\\
&= \int_{\ell_{t,\theta}} \phi(\|\mathbf{x}-\mathbf{y}\|^2)w(\|\mathbf{y}\|^2)\,\mathrm{d}\mathbf{y}\\
&= \int_{\ell_{t,0}} \phi(\|\mathbf{x}-Q_\theta\mathbf{y}\|^2)w(\|Q_\theta\mathbf{y}\|^2)\,\mathrm{d}\mathbf{y}\\
&= \int_{\ell_{t,0}} \phi(\|Q_\theta^{-1}\mathbf{x}-\mathbf{y}\|^2)w(\|\mathbf{y}\|^2)\,\mathrm{d}\mathbf{y}\\
&= \int_{\ell_{t,0}} \phi(\|\mathbf{x}_\theta-\mathbf{y}\|^2)w(\|\mathbf{y}\|^2)\,\mathrm{d}\mathbf{y},
\end{aligned}$$

with the rotation matrix

$$Q_\theta = \begin{bmatrix} \cos(\theta) & -\sin(\theta) \\ \sin(\theta) & \cos(\theta) \end{bmatrix} = \left[\mathbf{n}_\theta | \mathbf{n}_\theta^\perp\right] \qquad \text{for } \theta \in [0, \pi),$$

and perpendicular vectors

$$\mathbf{n}_\theta = \begin{bmatrix} \cos(\theta) \\ \sin(\theta) \end{bmatrix} \quad \text{and} \quad \mathbf{n}_\theta^\perp = \begin{bmatrix} -\sin(\theta) \\ \cos(\theta) \end{bmatrix},$$

where we let $\mathbf{x}_\theta = Q_\theta^{-1}\mathbf{x} = Q_\theta^T\mathbf{x}$, so that $\mathbf{x}_\theta = [\mathbf{x}^T\mathbf{n}_\theta, \mathbf{x}^T\mathbf{n}_\theta^\perp]^T \in \mathbb{R}^2$.

Note that any $\mathbf{y} \in \ell_{t,0}$ has the form $\mathbf{y} = [t, s]^T \in \mathbb{R}^2$ for parameter $s \in \mathbb{R}$. In the following, it will be convenient to let $\mathbf{v}_{t,s} := [t, s]^T = \mathbf{y}$ for $t, s \in \mathbb{R}$. This way, we obtain the representation

$$\begin{aligned} h_{t,\theta}(\mathbf{x}) &= \int_{\ell_{t,0}} \phi(\|\mathbf{x}_\theta - \mathbf{y}\|^2) w(\|\mathbf{y}\|^2)\, \mathrm{d}\mathbf{y} \\ &= \int_{\mathbb{R}} \phi(\|\mathbf{x}_\theta\|^2 - 2\mathbf{x}_\theta^T\mathbf{v}_{t,s} + \|\mathbf{v}_{t,s}\|^2) w(\|\mathbf{v}_{t,s}\|^2)\, \mathrm{d}s \\ &= \int_{\mathbb{R}} \phi(\|\mathbf{x}\|^2 - 2\mathbf{x}_\theta^T\mathbf{v}_{t,s} + \|\mathbf{v}_{t,s}\|^2) w(\|\mathbf{v}_{t,s}\|^2)\, \mathrm{d}s \\ &= \int_{\mathbb{R}} \phi\left((\mathbf{x}^T\mathbf{n}_\theta - t)^2 + (\mathbf{x}^T\mathbf{n}_\theta^\perp - s)^2\right) w(\|\mathbf{v}_{t,s}\|^2)\, \mathrm{d}s, \end{aligned}$$

where we have used the identity

$$\begin{aligned} &\|\mathbf{x}\|^2 - 2\mathbf{x}_\theta^T\mathbf{v}_{t,s} + \|\mathbf{v}_{t,s}\|^2 \\ &= \|\mathbf{x}\|^2 \pm (\mathbf{x}^T\mathbf{n}_\theta)^2 - 2\mathbf{x}^T\mathbf{n}_\theta t + t^2 \pm (\mathbf{x}^T\mathbf{n}_\theta^\perp)^2 - 2\mathbf{x}^T\mathbf{n}_\theta^\perp s + s^2 \\ &= \|\mathbf{x}\|^2 + \left(\mathbf{x}^T\mathbf{n}_\theta - t\right)^2 + \left(\mathbf{x}^T\mathbf{n}_\theta^\perp - s\right)^2 - \left[(\mathbf{x}^T\mathbf{n}_\theta)^2 + (\mathbf{x}^T\mathbf{n}_\theta^\perp)^2\right] \\ &= \left(\mathbf{x}^T\mathbf{n}_\theta - t\right)^2 + \left(\mathbf{x}^T\mathbf{n}_\theta^\perp - s\right)^2. \end{aligned}$$

We conclude the discussion of this subsection as follows.

Proposition 3 *The weighted basis functions $g_{t,\theta} : \mathbb{R}^2 \to \mathbb{R}$ in (19) can be represented as*

$$g_{t,\theta}(\mathbf{x}) = \int_{\mathbb{R}} \phi\left((\mathbf{x}^T\mathbf{n}_\theta - t)^2 + (\mathbf{x}^T\mathbf{n}_\theta^\perp - s)^2\right) w(\|\mathbf{v}_{t,s}\|^2)\, ds \cdot w(\|\mathbf{x}\|^2).$$

For $(\phi w)(|\cdot|^2) \in \mathrm{L}^1([0,\infty), \mathbb{R})$, $g_{t,\theta}(\mathbf{x})$ is for any $\mathbf{x} \in \mathbb{R}^2$ well-defined. □

3.2 Representation of the Matrix Entries

To solve the reconstruction problem

$$\mathcal{R}_{\mathcal{L}}(g) = \mathcal{R}_{\mathcal{L}}(f) \qquad \text{for } \mathcal{L} = \{\ell_1, \dots, \ell_n\} \subset \mathbb{R}^2\,,$$

this requires solving the linear system (6) with matrix entries a_{kj} as in (18), i.e.,

$$a_{kj} = \mathcal{R}^{\mathbf{x}}_{\ell_j}\left[\mathcal{R}^{\mathbf{y}}_{\ell_k}\left[\phi(\|\mathbf{x}-\mathbf{y}\|^2)w(\|\mathbf{y}\|^2)\right]\cdot w(\|\mathbf{x}\|^2)\right]. \tag{20}$$

In our following computations, we let $\ell_k := \ell_{t,\theta}$ and $\ell_j := \ell_{r,\varphi}$ to indicate the dependence on the Radon lines' parameters $(t,\theta),(r,\varphi) \in \mathbb{R}\times[0,\pi)$. Therefore, by using the representation of the weighted basis functions $g_{t,\theta}$ in Proposition 3, any matrix entry a_{kj} in (20) has the form

$$\begin{aligned} a_{kj} &= \mathcal{R}^{\mathbf{x}}_{\ell_{r,\varphi}}\left[g_{t,\theta}(\mathbf{x})\right] \qquad (21)\\ &= \int_{\ell_{r,\varphi}}\left[\int_{\mathbb{R}}\phi\left((\mathbf{x}^T\mathbf{n}_\theta - t)^2 + (\mathbf{x}^T\mathbf{n}_\theta^\perp - s)^2\right)w(\|\mathbf{v}_{t,s}\|^2)\,\mathrm{d}s\right]w(\|\mathbf{x}\|^2)\,\mathrm{d}\mathbf{x}. \end{aligned}$$

Now the line integral of $g_{t,\theta}$ over $\ell_{r,\varphi}$ can be transformed into a line integral over $\ell_{r,0}$, so that we obtain for a_{kj} in (21) the representation

$$\begin{aligned} &\int_{\ell_{r,\varphi}}\left[\int_{\mathbb{R}}\phi\left((\mathbf{x}^T\mathbf{n}_\theta - t)^2 + (\mathbf{x}^T\mathbf{n}_\theta^\perp - s)^2\right)w(\|\mathbf{v}_{t,s}\|^2)\,\mathrm{d}s\right]w(\|\mathbf{x}\|^2)\,\mathrm{d}\mathbf{x}\\ &= \int_{\ell_{r,0}}\left[\int_{\mathbb{R}}\phi\left((\mathbf{x}^TQ_\varphi^T\mathbf{n}_\theta - t)^2 + (\mathbf{x}^TQ_\varphi^T\mathbf{n}_\theta^\perp - s)^2\right)w(\|\mathbf{v}_{t,s}\|^2)\,\mathrm{d}s\right]w(\|\mathbf{x}\|^2)\,\mathrm{d}\mathbf{x}\\ &= \int_{\ell_{r,0}}\left[\int_{\mathbb{R}}\phi\left((\mathbf{x}^T\mathbf{n}_{\theta-\varphi} - t)^2 + (\mathbf{x}^T\mathbf{n}_{\theta-\varphi}^\perp - s)^2\right)w(\|\mathbf{v}_{t,s}\|^2)\,\mathrm{d}s\right]w(\|\mathbf{x}\|^2)\,\mathrm{d}\mathbf{x}\\ &= \int_{\mathbb{R}}\left[\int_{\mathbb{R}}\phi\left((\mathbf{v}_{r,\tilde{s}}^T\mathbf{n}_{\theta-\varphi} - t)^2 + (\mathbf{v}_{r,\tilde{s}}^T\mathbf{n}_{\theta-\varphi}^\perp - s)^2\right)w(\|\mathbf{v}_{t,s}\|^2)\,\mathrm{d}s\right]w(\|\mathbf{v}_{r,\tilde{s}}\|^2)\,\mathrm{d}\tilde{s}, \end{aligned}$$

where we let $\mathbf{x} = (r,\tilde{s})^T = \mathbf{v}_{r,\tilde{s}}$.

Now, since

$$\begin{aligned} &(\mathbf{v}_{r,\tilde{s}}^T\mathbf{n}_{\theta-\varphi} - t)^2 + (\mathbf{v}_{r,\tilde{s}}^T\mathbf{n}_{\theta-\varphi}^\perp - s)^2\\ &= (\mathbf{v}_{r,\tilde{s}}^T\mathbf{n}_{\theta-\varphi})^2 + (\mathbf{v}_{r,\tilde{s}}^T\mathbf{n}_{\theta-\varphi}^\perp)^2 - 2\mathbf{v}_{r,\tilde{s}}^T(\mathbf{n}_{\theta-\varphi}t + \mathbf{n}_{\theta-\varphi}^\perp s) + t^2 + s^2\\ &= \|\mathbf{v}_{r,\tilde{s}}\|^2 - 2\mathbf{v}_{r,\tilde{s}}^TQ_{\theta-\varphi}\mathbf{v}_{t,s} + \|\mathbf{v}_{t,s}\|^2\\ &= \|Q_\varphi\mathbf{v}_{r,\tilde{s}}\|^2 - 2(Q_\varphi\mathbf{v}_{r,\tilde{s}})^T(Q_\theta\mathbf{v}_{t,s}) + \|Q_\theta\mathbf{v}_{t,s}\|^2\\ &= \|Q_\varphi\mathbf{v}_{r,\tilde{s}} - Q_\theta\mathbf{v}_{t,s}\|^2, \end{aligned}$$

we can conclude the discussion of this section as follows.

Proposition 4 *Let $K_{\phi,w}(\mathbf{x},\mathbf{y})$ be a weighted kernel of the form (12), where $(\phi w)(|\cdot|^2) \in \mathrm{L}^1(\mathbb{R})$. Then, all entries of the symmetric positive definite kernel matrix $A_{K,\mathcal{L}} = (a_{kj})_{1\le k,j\le n} \in \mathbb{R}^{n\times n}$ in (16) are well-defined, where the matrix entry a_{kj} in (18) is given as*

$$a_{kj} = \int_{\mathbb{R}}\int_{\mathbb{R}} \phi\left(\|Q_\varphi \mathbf{v}_{r,\tilde{s}} - Q_\theta \mathbf{v}_{t,s}\|^2\right) w(\|\mathbf{v}_{t,s}\|^2) w(\|\mathbf{v}_{r,\tilde{s}}\|^2)\,\mathrm{d}s\,\mathrm{d}\tilde{s}.$$

In particular, we have the representation

$$a_{kk} = \int_{\mathbb{R}}\int_{\mathbb{R}} \phi\left((\tilde{s}-s)^2\right) w(t^2+s^2) w(\tilde{s}^2+r^2)\,\mathrm{d}s\,\mathrm{d}\tilde{s}$$

for the diagonal entries of the matrix $A_{K,\mathcal{L}}$. □

4 Special Case: Gaussian Kernel and Gaussian Weight

In our numerical experiments, we considered using the special case, where $K_{\phi,w}(\mathbf{x},\mathbf{y})$ in (12) is given by a combination of the Gaussian kernel

$$\phi_\alpha(\|\mathbf{x}-\mathbf{y}\|^2) = \mathrm{e}^{-\alpha\|\mathbf{x}-\mathbf{y}\|^2} \qquad \text{for } \mathbf{x},\mathbf{y}\in\mathbb{R}^2 \text{ and } \alpha>0$$

and the Gaussian weight function

$$w_\beta(\|\mathbf{x}\|^2) = \mathrm{e}^{-\beta\|\mathbf{x}\|^2} \qquad \text{for } \mathbf{x}\in\mathbb{R}^2 \text{ and } \beta>0.$$

For the purposes of this paper, it is quite instructive to show how we computed the weighted Gaussian basis functions $g_{t,\theta}$ in Proposition 3 and the Gaussian matrix entries a_{kj} in Proposition 4 for this prototypical case. For other special cases, explicit representations for weighted basis functions $g_{t,\theta}$ and matrix entries a_{kj} should be elaborated by following along the lines of our following computations.

4.1 Weighted Gaussian Basis Functions

Starting from the representation of $g_{t,\theta}(\mathbf{x})$ in Proposition 3, we obtain

$$\begin{aligned}
&g_{t,\theta}(\mathbf{x})\\
&= \int_{\mathbb{R}} \mathrm{e}^{-\alpha\left[(\mathbf{x}^T\mathbf{n}_\theta - t)^2 + (\mathbf{x}^T\mathbf{n}_\theta^\perp - s)^2\right]} \mathrm{e}^{-\beta(t^2+s^2)}\,\mathrm{d}s \cdot \mathrm{e}^{-\beta\|x\|^2}\\
&= \mathrm{e}^{-\alpha\left[(\mathbf{x}^T\mathbf{n}_\theta - t)^2 + (\mathbf{x}^T\mathbf{n}_\theta^\perp)^2\right] - \beta(t^2+\|x\|^2)} \int_{\mathbb{R}} \mathrm{e}^{-\alpha\left[-2(\mathbf{x}^T\mathbf{n}_\theta^\perp)s + s^2\right] - \beta s^2}\,\mathrm{d}s\\
&= \mathrm{e}^{-\left[(\alpha+\beta)t^2 + \alpha\left((\mathbf{x}^T\mathbf{n}_\theta)^2 + (\mathbf{x}^T\mathbf{n}_\theta^\perp)^2 - 2(\mathbf{x}^T\mathbf{n}_\theta)t\right) + \beta\|x\|^2\right]} \int_{\mathbb{R}} \mathrm{e}^{-\left[(\alpha+\beta)s^2 - 2\alpha(\mathbf{x}^T\mathbf{n}_\theta^\perp)s\right]}\,\mathrm{d}s\\
&= \mathrm{e}^{-\left[(\alpha+\beta)(t^2+\|x\|^2) - 2\alpha(\mathbf{x}^T\mathbf{n}_\theta)t\right]} \int_{\mathbb{R}} \mathrm{e}^{-\left[(\alpha+\beta)s^2 - 2\alpha(\mathbf{x}^T\mathbf{n}_\theta^\perp)s \pm \frac{\alpha^2}{\sqrt{\alpha+\beta}}(\mathbf{x}^T\mathbf{n}_\theta^\perp)^2\right]}\,\mathrm{d}s\\
&= \mathrm{e}^{-\left[(\alpha+\beta)(t^2+\|x\|^2) - 2\alpha(\mathbf{x}^T\mathbf{n}_\theta)t - \frac{\alpha^2}{\alpha+\beta}(\mathbf{x}^T\mathbf{n}_\theta^\perp)^2\right]} \int_{\mathbb{R}} \mathrm{e}^{-\left[\sqrt{\alpha+\beta}s - \frac{\alpha}{\sqrt{\alpha+\beta}}(\mathbf{x}^T\mathbf{n}_\theta^\perp)\right]^2}\,\mathrm{d}s,
\end{aligned}$$

so that we can draw the following conclusion.

Proposition 5 *For $(t,\theta) \in \mathbb{R} \times [0,\pi)$, the weighted Gaussian basis functions are given as*

$$g_{t,\theta}(\mathbf{x}) = \sqrt{\frac{\pi}{\alpha+\beta}} \cdot e^{-\left[(\alpha+\beta)(t^2+\|x\|^2)-2\alpha(\mathbf{x}^T\mathbf{n}_\theta)t-\frac{\alpha^2}{\alpha+\beta}(\mathbf{x}^T\mathbf{n}_\theta^\perp)^2\right]} \quad \text{for } \mathbf{x} \in \mathbb{R}^2,$$

where $\alpha, \beta > 0$. □

4.2 Gaussian Matrix Entries

To compute the entries a_{kj} of the Gaussian kernel matrix, we can rely on the following standard result from basic calculus.

Lemma 1 *For $c_0, c_1 \in \mathbb{R}$ and $c_2 > 0$, we have*

$$\int_{\mathbb{R}} \mathrm{e}^{-\left[c_0+c_1 s+c_2 s^2\right]} \,\mathrm{d}s = \sqrt{\frac{\pi}{c_2}}\, \mathrm{e}^{\frac{c_1^2}{4c_2}-c_0}.$$

Proof By completion of the square in the exponent of the integrand, we get

$$\int_{\mathbb{R}} \mathrm{e}^{-\left[c_0+c_1 s+c_2 s^2\right]} \,\mathrm{d}s = \int_{\mathbb{R}} \mathrm{e}^{-\left[c_0+\left(\frac{c_1}{2\sqrt{c_2}}+\sqrt{c_2}s\right)^2-\frac{c_1^2}{4c_2}\right]} \,\mathrm{d}s = \sqrt{\frac{\pi}{c_2}}\, \mathrm{e}^{\frac{c_1^2}{4c_2}-c_0},$$

where we have used the substitution $u = \frac{c_1}{2\sqrt{c_2}} + \sqrt{c_2}s$. □

Now we are in a position where we can compute the entries a_{kj} of the Gaussian matrix by using their representation in Proposition 4. To this end, we use similar calculations as in the outset of Section 3.2. We recall the representation $\mathbf{v}_{r,s} = (r,s)^T \in \mathbb{R}^2$ for a point on line $\ell_{r,0}$. Moreover, recall that for two perpendicular unit vectors $\mathbf{n}_\theta$ and $\mathbf{n}_\theta^\perp$ their rotation about angle $-\varphi$ is given by $Q_\varphi^T \mathbf{n}_\theta = \mathbf{n}_{\theta-\varphi}$ and $Q_\varphi^T \mathbf{n}_\theta^\perp = \mathbf{n}_{\theta-\varphi}^\perp$, respectively. This then yields

$$\begin{aligned} a_{kj} &= \int_{\ell_{r,\varphi}} \sqrt{\frac{\pi}{\alpha+\beta}} \mathrm{e}^{-\left[(\alpha+\beta)(t^2+\|x\|^2)-2\alpha(\mathbf{x}^T\mathbf{n}_\theta)t-\frac{\alpha^2}{\alpha+\beta}(\mathbf{x}^T\mathbf{n}_\theta^\perp)^2\right]} \,\mathrm{d}x \\ &= \sqrt{\frac{\pi}{\alpha+\beta}} \int_{\ell_{r,0}} \mathrm{e}^{-\left[(\alpha+\beta)(t^2+\|x\|^2)-2\alpha((Q_\varphi\mathbf{x})^T\mathbf{n}_\theta)t-\frac{\alpha^2}{\alpha+\beta}((Q_\varphi\mathbf{x})^T\mathbf{n}_\theta^\perp)^2\right]} \,\mathrm{d}x \\ &= \sqrt{\frac{\pi}{\alpha+\beta}} \int_{\mathbb{R}} \mathrm{e}^{-\left[(\alpha+\beta)(t^2+r^2+s^2)-2\alpha t(\mathbf{v}_{r,s}^T\mathbf{n}_{\theta-\varphi})-\frac{\alpha^2}{\alpha+\beta}(\mathbf{v}_{rs}^T\mathbf{n}_{\theta-\varphi}^\perp)^2\right]} \,\mathrm{d}s. \quad (22) \end{aligned}$$

With letting $\eta = \theta - \varphi$, and by using

$$\mathbf{v}_{r,s}^T\mathbf{n}_\eta = r\cos(\eta) + s\sin(\eta) \quad \text{and} \quad \mathbf{v}_{r,s}^T\mathbf{n}_\eta^\perp = s\cos(\eta) - r\sin(\eta),$$

we can rewrite the exponent in the integrand in (22) as

$$c_0 + c_1 s + c_2 s^2,$$

where we let

$$c_0 \equiv c_0(r,t,\eta) = (\alpha+\beta)(r^2+t^2) - 2\alpha rt\cos(\eta) - \frac{\alpha^2}{\alpha+\beta} r^2\sin^2(\eta)$$
$$c_1 \equiv c_1(r,t,\eta) = 2\alpha\sin(\eta)\left(\frac{\alpha}{\alpha+\beta} r\cos(\eta) - t\right)$$
$$c_2 \equiv c_2(\eta) = \alpha+\beta - \frac{\alpha^2}{\alpha+\beta}\cos^2(\eta).$$

Now note that c_2 is positive for any $\eta \in \mathbb{R}$,

$$c_2 = \alpha+\beta - \frac{\alpha^2}{\alpha+\beta}\cos^2(\eta) \geq \alpha+\beta - \frac{\alpha^2}{\alpha+\beta} = \frac{\beta(\beta+2\alpha)}{\alpha+\beta} > 0,$$

so that we can rely on Lemma 1 to obtain the representation

$$a_{kj} = \frac{\pi}{\sqrt{(\alpha+\beta)c_2}}\, \mathrm{e}^{\frac{c_1^2}{4c_2} - c_0}. \tag{23}$$

For the purpose of implementation, the following representation for the matrix entries is quite convenient.

Proposition 6 *The entries of the Gaussian matrix $A_{K,\mathcal{L}}$ in* (16) *are given as*

$$a_{kj} = \frac{\pi}{\sqrt{q_{\alpha,\beta}(\eta)}} \exp\left(-\beta(2\alpha+\beta)\cdot \frac{p_{\alpha,\beta}(t,r,\eta)}{q_{\alpha,\beta}(\eta)}\right), \tag{24}$$

where $\eta = \theta - \varphi$ and where

$$p_{\alpha,\beta}(t,r,\eta) = (\alpha+\beta)(r^2+t^2) - 2\alpha rt\cos(\eta)$$
$$q_{\alpha,\beta}(\eta) = (\alpha+\beta)^2 - \alpha^2\cos^2(\eta).$$

Moreover, the matrix $A_{K,\mathcal{L}}$ is symmetric positive definite with diagonal entries

$$a_{kk} = \frac{\pi}{\sqrt{\beta(2\alpha+\beta)}}\, \mathrm{e}^{-2\beta t^2} > 0 \qquad \text{for any } (t,\theta) \in \mathbb{R}\times[0,\pi). \tag{25}$$

Proof Starting from the representation in (23), first note that

$$q_{\alpha,\beta}(\eta) = (\alpha+\beta)c_2.$$

Therefore, it remains to show the identity

$$\frac{c_1^2}{4c_2} - c_0 = -\beta(2\alpha+\beta)\cdot\frac{p_{\alpha,\beta}(t,r,\eta)}{q_{\alpha,\beta}(\eta)},$$

or, equivalently,

$$q_{\alpha,\beta}(\eta)\left(\frac{c_1^2}{4c_2} - c_0\right) = -\beta(2\alpha+\beta)\cdot p_{\alpha,\beta}(t,r,\eta). \tag{26}$$

To establish (26), we first represent the right hand side in (26) by

$$\begin{aligned}
&-\beta(2\alpha+\beta)\cdot p_{\alpha,\beta}(t,r,\eta)\\
&=-\beta(2\alpha+\beta)\left[(\alpha+\beta)(r^2+t^2)-2\alpha rt\cos(\eta)\right]\\
&=2\alpha\beta(2\alpha+\beta)\cos(\eta)rt-\beta(2\alpha+\beta)(\alpha+\beta)(r^2+t^2). \qquad (27)
\end{aligned}$$

Now let us turn to the left hand side of (26). Note that

$$\begin{aligned}
\frac{c_1^2}{4}&=\alpha^2\sin^2(\eta)\left[\frac{\alpha^2}{(\alpha+\beta)^2}\cos^2(\eta)r^2-2\frac{\alpha}{\alpha+\beta}\cos(\eta)rt+t^2\right]\\
&=\frac{\alpha^4}{(\alpha+\beta)^2}\cos^2(\eta)\sin^2(\eta)r^2-2\frac{\alpha^3}{\alpha+\beta}\cos(\eta)\sin^2(\eta)rt+\alpha^2\sin^2(\eta)t^2.
\end{aligned}$$

This in combination with $q_{\alpha,\beta}(\eta)/c_2=\alpha+\beta$ yields

$$\frac{q_{\alpha,\beta}(\eta)}{c_2}\frac{c_1^2}{4}=\frac{\alpha^4\cos^2(\eta)\sin^2(\eta)}{\alpha+\beta}r^2-2\alpha^3\cos(\eta)\sin^2(\eta)rt+\alpha^2(\alpha+\beta)\sin^2(\eta)t^2.$$

Moreover, we find

$$\begin{aligned}
&q_{\alpha,\beta}(\eta)\cdot c_0\\
&=\left[(\alpha+\beta)^2-\alpha^2\cos^2(\eta)\right]\left[(\alpha+\beta)(r^2+t^2)-2\alpha\cos(\eta)rt-\frac{\alpha^2}{\alpha+\beta}\sin^2(\eta)r^2\right]\\
&=(\alpha+\beta)^3(r^2+t^2)-2\alpha(\alpha+\beta)^2\cos(\eta)rt-\alpha^2(\alpha+\beta)\sin^2(\eta)r^2\\
&\quad-\alpha^2(\alpha+\beta)\cos^2(\eta)(r^2+t^2)+2\alpha^3\cos^3(\eta)rt+\frac{\alpha^4}{\alpha+\beta}\cos^2(\eta)\sin^2(\eta)r^2\\
&=\left[(\alpha+\beta)^3-\alpha^2(\alpha+\beta)+\frac{\alpha^4}{\alpha+\beta}\cos^2(\eta)\sin^2(\eta)\right]r^2\\
&\quad+2\alpha\cos(\eta)\left[\alpha^2\cos^2(\eta)-(\alpha+\beta)^2\right]rt+\left[(\alpha+\beta)^3-\alpha^2(\alpha+\beta)\cos^2(\eta)\right]t^2.
\end{aligned}$$

This leads us to the representation

$$\begin{aligned}
&q_{\alpha,\beta}(\eta)\cdot\left(\frac{c_1^2}{4c_2}-c_0\right)\\
&=\left[\frac{\alpha^4}{\alpha+\beta}\cos^2(\eta)\sin^2(\eta)-(\alpha+\beta)^3+\alpha^2(\alpha+\beta)-\frac{\alpha^4}{\alpha+\beta}\cos^2(\eta)\sin^2(\eta)\right]r^2\\
&\quad+2\alpha\cos(\eta)\left[(\alpha+\beta)^2-\alpha^2\sin^2(\eta)-\alpha^2\cos^2(\eta)\right]rt\\
&\quad+\left[\alpha^2(\alpha+\beta)\sin^2(\eta)-(\alpha+\beta)^3+\alpha^2(\alpha+\beta)\cos^2(\eta)\right]t^2\\
&=\left[\alpha^2(\alpha+\beta)-(\alpha+\beta)^3\right](r^2+t^2)+2\alpha\cos(\eta)\left[(\alpha+\beta)^2-\alpha^2\right]rt\\
&=2\alpha\beta(2\alpha+\beta)\cos(\eta)rt-\beta(2\alpha+\beta)(\alpha+\beta)(r^2+t^2)
\end{aligned}$$

for the left hand side in (26), which coincides with the right hand side in (27).

The stated symmetry of the Gaussian matrix $A_{K,\mathcal{L}}$ is due to the symmetry of the functions $q_{\alpha,\beta}$ and $p_{\alpha,\beta}$ in (24), where we can in particular rely on

$$\begin{aligned} q_{\alpha,\beta}(\eta) &= q_{\alpha,\beta}(-\eta) \quad \text{for all } \eta \in \mathbb{R} \\ p_{\alpha,\beta}(t,r,\eta) &= p_{\alpha,\beta}(t,r,-\eta) \quad \text{for all } r,t,\eta \in \mathbb{R} \\ p_{\alpha,\beta}(t,r,\eta) &= p_{\alpha,\beta}(r,t,\eta) \quad \text{for all } r,t,\eta \in \mathbb{R}, \end{aligned}$$

so that, by using representation (24), we get

$$\begin{aligned} a_{kj} &= \frac{\pi}{\sqrt{q_{\alpha,\beta}(\eta)}} \exp\left(-\beta(2\alpha+\beta)\cdot\frac{p_{\alpha,\beta}(t,r,\eta)}{q_{\alpha,\beta}(\eta)}\right) \\ &= \frac{\pi}{\sqrt{q_{\alpha,\beta}(-\eta)}} \exp\left(-\beta(2\alpha+\beta)\cdot\frac{p_{\alpha,\beta}(r,t,-\eta)}{q_{\alpha,\beta}(-\eta)}\right) = a_{jk}. \end{aligned}$$

Let us finally turn to the diagonal entries a_{kk}. In this case, $\eta = \theta - \varphi = 0$ and $r = t$, so that due to

$$\begin{aligned} q_{\alpha,\beta}(0) &= \beta(2\alpha+1) \\ p_{\alpha,\beta}(t,t,0) &= 2\beta t^2. \end{aligned}$$

we obtain the stated representation (25). □

5 Numerical Examples

We have implemented the proposed kernel-based reconstruction scheme for the weighted Gaussian kernel

$$K_{\phi,w}(\mathbf{x},\mathbf{y}) = \phi_\alpha\left(\|\mathbf{x}-\mathbf{y}\|^2\right)\cdot w_\beta(\|\mathbf{x}\|^2)\cdot w_\beta(\|\mathbf{y}\|^2) \qquad \text{for } \alpha,\beta>0$$

by using the Gaussian kernel

$$\phi_\alpha(\|\mathbf{x}-\mathbf{y}\|^2) = \mathrm{e}^{-\alpha\|\mathbf{x}-\mathbf{y}\|^2} \qquad \text{for } \alpha>0$$

in combination with the Gaussian weight function

$$w_\beta(\|\mathbf{x}\|^2) = \mathrm{e}^{-\beta\|\mathbf{x}\|^2} \qquad \text{for } \beta>0.$$

For the purpose of illustration, we considered applying the proposed kernel-based reconstruction method to two popular phantoms:

(a) The phantom `bull's eye`, $f_{\mathrm{BE}} : [-1,1]^2 \to \mathbb{R}$, given as a linear combination

$$f_{\mathrm{BE}}(\mathbf{x}) = \chi_{B_{3/4}}(\mathbf{x}) - \frac{3}{4}\chi_{B_{1/2}}(\mathbf{x}) + \frac{1}{4}\chi_{B_{1/4}}(\mathbf{x}) \qquad \text{for } \mathbf{x}\in[-1,1]^2 \quad (28)$$

of three indicator functions χ_{B_r} on the disks (each centred at the origin $\mathbf{0}$)

$$B_r = \left\{\mathbf{x}\in\mathbb{R}^2 : \|\mathbf{x}\| \le r\right\} \qquad \text{for } r = 3/4, 1/2, 1/4.$$

The phantom bull's eye is shown in Figure 1 (top left).

(b) The `crescent-shaped` phantom $f_{\mathrm{CS}} : [-1,1]^2 \to \mathbb{R}$ is defined as

$$f_{\mathrm{CS}}(\mathbf{x}) = \chi_{B_{1/2}}(\mathbf{x}) - \frac{1}{2}\chi_{B_{3/8}(1/8,0)}(\mathbf{x}) \qquad \text{for } \mathbf{x} \in [-1,1]^2, \tag{29}$$

where

$$B_{3/8}(1/8,0) = \left\{\mathbf{x} = (x,y) \in \mathbb{R}^2 : (x-1/8)^2 + y^2 \le 9/64\right\}$$

is the disk of radius $3/8$ centred at $(1/8, 0)$. The crescent-shaped phantom is shown in Figure 1 (top right). Note that f_{CS} is *not* radially symmetric, unlike f_{BE}.

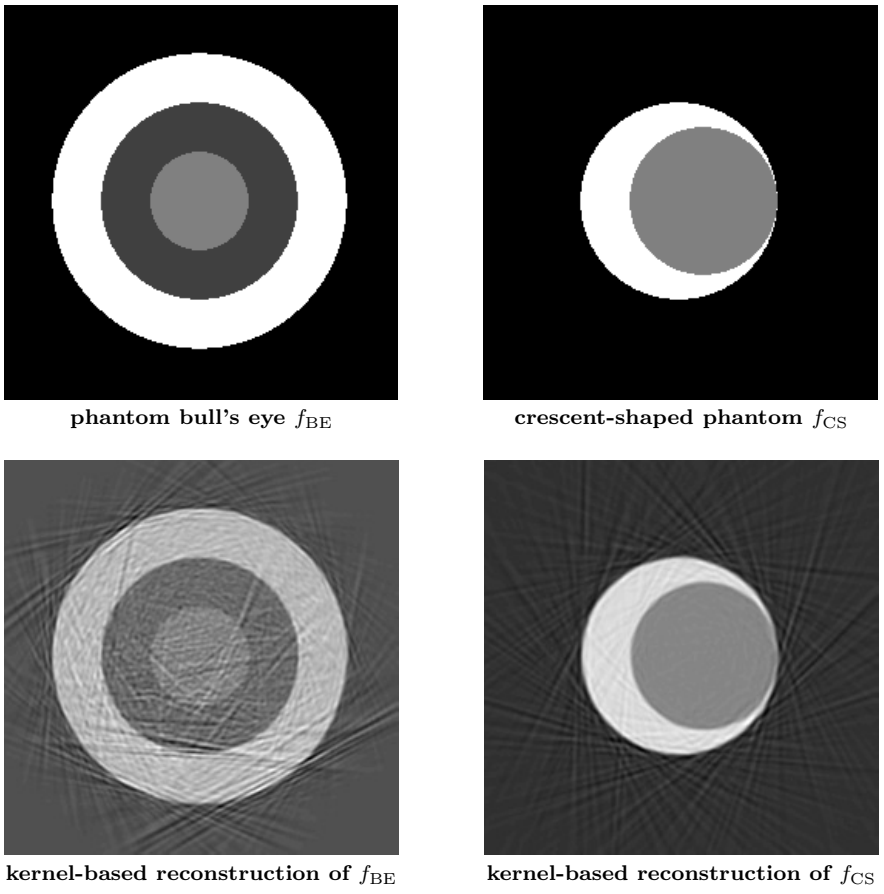

Fig. 1 Reconstruction of two phantoms by weighted Gaussian kernel functions. (a) `bull's eye`, as defined by f_{BE} in (28); (b) `crescent-shaped`, given as f_{CS} in (29). The reconstruction quality is further evaluated by MSE, PSNR, SSIM, cf. our results in Table 1.

For each test case, we acquired scattered Radon data $\{(\mathcal{R}f)(t_k,\theta_k)\}_{1\le k\le n}$ by line integrals of f over $n = 16,384$ scattered Radon lines $\{\ell_{t_k,\theta_k}\}_{1\le k\le n}$. To this end, we randomly chose line parameters $(t_k,\theta_k) \in [-\sqrt{2},\sqrt{2}] \times [0,\pi)$, for $1 \le k \le n$.

We measured the quality of our reconstruction g by the *mean square error*

$$\mathrm{MSE} = \frac{1}{J}\sum_{j=1}^{J}(f_j - g_j)^2,$$

where J is the size of the input image (i.e., the number of pixels), and where $f \equiv \{f_j\}_{j=1}^J$ and $g \equiv \{g_j\}_{j=1}^J$ are the greyscale values at the pixels of the target image f and of the reconstructed image g, respectively. In our numerical experiments, the image size is $J = 256 \times 256 = 65,536$. We remark that the MSE is by

$$\mathrm{PSNR} = 10 \times \log_{10}\left(\frac{(2^r-1)\times(2^r-1)}{\mathrm{MSE}}\right)$$

related to the *peak signal-to-noise ratio* (PSNR). In our numerical experiments, we have $r = 8$, giving the number of bits required for the representation of one luminance value.

Finally, we also recorded the *structural similarity index* (SSIM) to better measure the "similarity" between f and g. We remark that SSIM was designed in [14] to improve on the quality measures PSNR and MSE, particularly to obtain an enhanced consistency with human visual perception.

Our numerical results are shown in Figure 1 and in Table 1.

Table 1 Reconstruction of two phantoms by weighted Gaussian kernel functions.

phantom	α	β	MSE	PSNR	SSIM
`bull's eye`	`7.0711`	`1.5166`	`0.0151`	`66.3314`	`0.3338`
`crescent-shaped`	`7.0711`	`1.0954`	`0.0054`	`70.8376`	`0.4752`

We can conclude that the key features of the two test images are captured quite well by the proposed kernel-based reconstruction scheme. However, both their visual quality and their indicators MSE, PSNR, and SSIM may further be improved by fine-tuning the Gaussian shape parameters α and β. This, however, is far beyond the aims of this paper, and therefore we decided to refrain from optimizing the method parameters α and β.

Acknowledgement. The first author was supported by the project *"Multivariate approximation with application to image reconstruction"* of the University of Padova, years 2013-2014.

References

1. R.K. Beatson and W. zu Castell: Scattered data interpolation of Radon data. Calcolo **48**, 2011, 5–19.
2. Å. Bjørck: *Numerical Methods for Least Squares Problems*. SIAM, Philadelphia, 1996.
3. S. Bochner: *Vorlesungen über Fouriersche Integrale*. Akademische Verlagsgesellschaft, Leipzig, 1932.
4. S. De Marchi, A. Iske, and A. Sironi: Kernel-based image reconstruction from scattered Radon data. Dolomites Research Notes on Approximation **9**, 2016, 19–31.
5. T.G. Feeman: *The Mathematics of Medical Imaging. A Beginner's Guide*. Second Edition, Springer Undergraduate Texts in Mathematics and Technology. Springer, New York, 2015.
6. R. Gordon, R. Bender, and G. Herman: Algebraic reconstruction techniques (ART) for three dimensional electron microscopy and X-ray photography. Journal of Theoretical Biology **29**(3), 1970, 471–481.
7. S. Helgason: *The Radon Transform*. Progress in Mathematics, vol. 5, 2nd edition. Birkhäuser, Basel, 1999.
8. A. Iske: *Charakterisierung bedingt positiv definiter Funktionen für multivariate Interpolationsmethoden mit radialen Basisfunktionen*. Dissertation, University of Göttingen,1994.
9. A. Iske: Reconstruction of functions from generalized Hermite-Birkhoff data. In: *Approximation Theory VIII, Vol. 1: Approximation and Interpolation*, C.K. Chui and L.L. Schumaker (eds.), World Scientific, Singapore, 1995, 257–264.
10. A. Iske: Scattered data approximation by positive definite kernel functions. Rend. Sem. Mat. Univ. Pol. Torino **69**(3), 2011, 217–246.
11. F. Natterer: *The Mathematics of Computerized Tomography*. Classics in Applied Mathematics, vol. 32. SIAM, Philadelphia, 2001.
12. J. Radon: Über die Bestimmung von Funktionen durch ihre Integralwerte längs gewisser Mannigfaltigkeiten. Berichte Sächsische Akademie der Wissenschaften **69**, 1917, 262–277.
13. R. Schaback and H. Wendland: Characterization and construction of radial basis functions. *Multivariate Approximation and Applications*, N. Dyn, D. Leviatan, D. Levin, and A. Pinkus (eds.), Cambridge University Press, Cambridge, 2001, 1–24.
14. Z. Wang, A.C. Bovik, H.R. Sheikh, and E.P. Simoncelli: Image quality assessment: from error visibility to structural similarity. IEEE Transactions on Image Processing **13**(4), April 2004, 600–612.
15. H. Wendland: *Scattered Data Approximation*. Cambridge University Press, 2005.